Influence of orography and canopy conditions on friction velocity observed during frontal events using doppler sodar observations

V. Kotroni, Christine Amory-Mazaudier

Reprinted from JOURNAL OF APPLIED METEOROLOGY, Vol. 32, No. 3, March 1993
American Meteorological Society

Influence of Orographic and Canopy Conditions on Friction Velocities Observed during Frontal Events Using Doppler Sodar Observations

V. KOTRONI AND C. AMORY-MAZAUDIER

CRPE(CNET/CNRS), Saint-Maur des Fossés, France

(Manuscript received 28 March 1992, in final form 23 July 1992)

ABSTRACT

Sodar friction velocities, obtained during frontal events traversing areas characterized by different orographic and canopy conditions (flat, bare ground, small hills and valleys with agricultural crops and trees, agricultural crops and forest on a flat ground, bare ground on the side of a mountain), are compared in order to identify the influence of topography on this parameter. For some case studies, sounding and sodar data are combined in order to provide a relation between the friction velocity and the low-level jet presence. For the cases analyzed in this paper, the following results are obtained: the frontal passage is associated with a decrease of the horizontal wind speed (about 50% in magnitude) in the surface layer, and an increase of the friction velocity before the frontal passage followed by a decrease just at the time of the frontal passage or with a little delay. Friction velocity is more intense in the cold side of the low-level jet and its maximum represents 2% of the low-level jet maximum magnitude. As it concerns the influence of the terrain conditions on friction velocity, mountain effects yield to more intense friction-velocity values and to a superposition of an oscillating behavior on the time variation of friction velocity, while forest effects induce a shift of the frontal signature on the time variation of friction velocity at higher height levels.

1. Introduction

The importance of turbulent exchange processes in the atmospheric boundary layer to the general circulation of the atmosphere has long been recognized and it has been a central and recurring feature of much of micrometeorological research to establish means of deriving turbulent fluxes from wind speed and temperature profiles (Businger et al. 1971; Nieuwstadt 1978; Lo 1979; Byun 1990). In the surface layer, the terrain interactions with the wind field are characterized by the friction velocity u_* associated with the turbulent flux of vertical momentum transfer. In addition, friction velocity in the atmospheric surface layer plays an important role in numerical modeling of the planetary boundary layer (PBL). The PBL, in the presence of a frontal system, is frequently not taken into account in numerical modeling. Nevertheless, frontal occurrence modifies the normal evolution of PBL parameters (the major part of the ageostrophic circulation associated with a cold front is essentially confined in the PBL) and the understanding of these modifications associated with the frontal dynamics is vital to numerical modeling and weather forecasting (Ball 1960; Stone 1966; Hoskins and Bretherton 1972; Mak 1972; Keyser and Anthes 1982). Therefore, for a better understanding of the interactions between the PBL and surface frontal events, frontal friction over different terrain conditions is analyzed in this paper.

During the last decade, the CRPE (Centre de Recherches en Physique de l'Environnement) Doppler sodars were involved in four international campaigns (MESOGERS84, HAPEX–MOBILHY86, FRONTS87, PYREX90), which took place in various areas in France, characterized by different orographic and canopy conditions. From each of these international campaigns, one or two cases of cold fronts have been selected. The criterion for selection of frontal cases for the FRONTS87 experiment was the quality of the available data. For the other three campaigns, which did not principally aim at the study of fronts, the criterion was the coincidence of an intensive observation period with a frontal event. Friction velocities deduced from sodar measurements have been analyzed in connection with the variation of the horizontal wind speed (also measured by sodar) in the PBL. When sounding data were available, they were combined with sodar data to provide a relation between friction velocity time variation and the presence of the low-level jet associated with the frontal passage.

In the second section of this paper a brief description of the four experimental campaigns is given. Section 3 presents the main tool of this study, the CRPE Doppler sodar, followed by a description of the method used to derive friction velocity from the high-resolution (4-s) sodar raw data. The fourth section presents the

Corresponding author address: Vassiliki Kotroni, CNET/CRPE, 4, avenue de Neptune, Saint-Maur des Fossés, France 94107.

observations and the last two are devoted to the discussion of the results and the conclusions.

2. Datasets

During the last decade, four international campaigns involving sodar measurement took place in France (see Fig. 1) for various scientific purposes.

The MESOGERS84 field experiment (mesoscale experiment in the Gers region) was performed in southwestern France from 10 September to 5 October 1984 (described by Weill et al. 1988a). It was essentially designed to study mesoscale flow in the heterogeneous boundary layer. This campaign provided test data for parameterization schemes to be adopted in mesoscale numerical forecast models with special emphasis on momentum, sensible, and latent heat flux transfers at different scales, from a few kilometers up to 50 km. During this experiment, an array of instruments was distributed within the experimental area (a 50-km $\times$ 50-km square). The main studies that have been undertaken, concerned the analysis of fluxes at different temporal and spatial scales and the evolution of atmospheric flow over complex terrain toward a homogeneous flow (physical mechanisms interferring: plumes and thermals, mesoscale phenomena such as gravity waves and frontal systems).

The HAPEX–MOBILHY86 campaign (Hydrological–Atmospheric Pilot Experiment/Modélisation du Bilan Hydrique) took place also in the southwest of France from the beginning of May to the middle of July 1986 (described by André et al. 1988). Its main

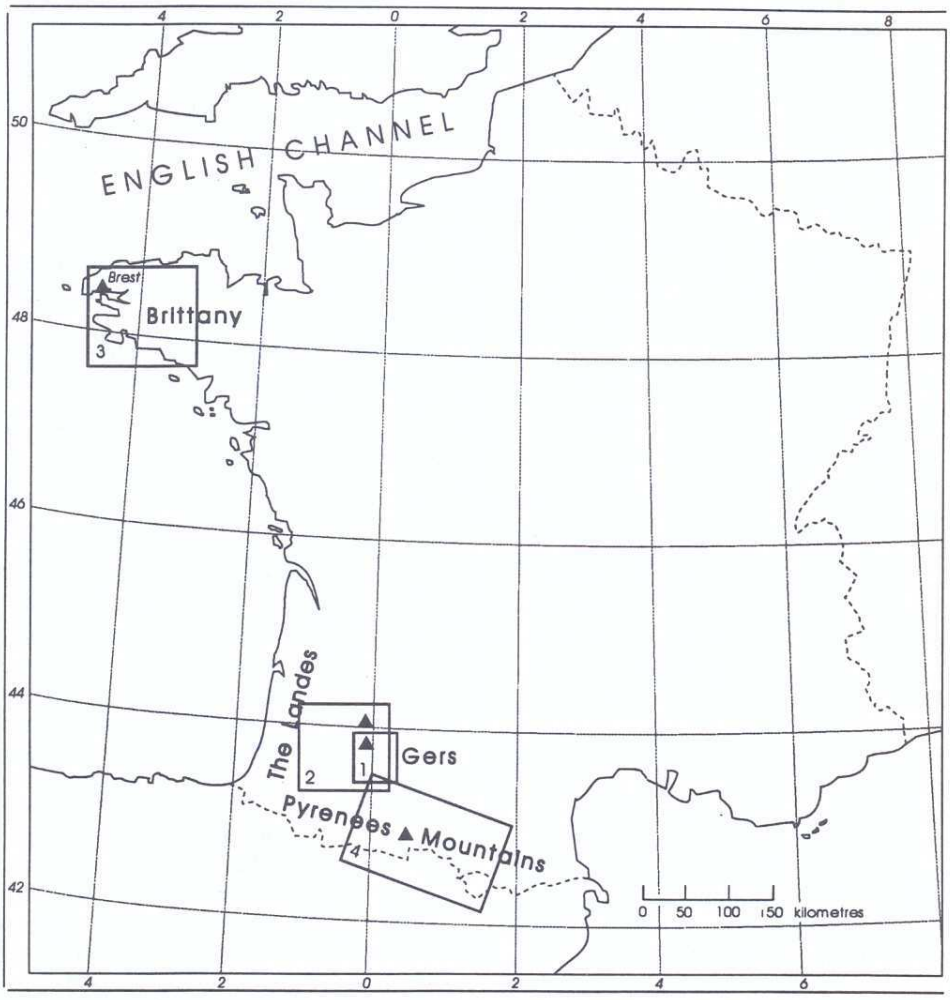

FIG. 1. Representation of the experimental areas corresponding to each campaign: box 1, for MESOGERS84; box 2, for HAPEX–MOBILHY86; box 3, for FRONTS87; box 4, for PYREX90. For the last two campaigns the boxes represent only the inner part of the experimental area. Triangles (in the boxes) denote the acoustic sounder site.

goal was to document the hydrological balance and evaporative fluxes over crops and forested areas. The experimental site was a square area of 100 km × 100 km, with pine forest over one-half and agricultural crops over the other half. The undertaken studies concerned mostly (i) the analysis of spatial variability of evaporative fluxes due to climatic, hydrologic, and pedologic conditions, and to different vegetative canopies, and (ii) the improvement of realism and accuracy of mesoscale models to provide detailed and spatially varying surface conditions.

The FRONTS87/Mesoscale Frontal Dynamics Project was a European experiment that lasted from 18 October 1987 until 13 January 1988 and aimed at studying the dynamics of the active cold fronts observed over the area centered on the Channel between England and France (Clough 1987). The FRONTS87 experimental area consisted of a threefold nested structure, covering synoptic, mesoscale and microscale measurements. Studies concerning the different dynamic mechanisms resulting in the formation of precipitations have been undertaken, using the data provided from this campaign.

The main scientific goal of PYREX90 (Pyrenees Experiment), which took place during a 2-month period (October and November 1990), was to establish a database for several detailed studies of the dynamic influence of a large and fairly simple mountain range, like the Pyrenees Mountains, over the atmosphere (Bougeault 1990). A large number of measurements were concentrated along a vertical cross section perpendicular to the mountain range in its central part.

The major part of the data used in this study are provided by the Doppler sodar, and they are combined, when available, with sounding data. All four campaigns were conceived and performed during the last decade and provided measurements over four different terrain conditions. This is very important for an objective study and analysis of friction velocity during frontal events under the influence of different topographic characteristics. Table 1 gives, for all four experiments, the geographic, orographic, and canopy characteristics of the sodar site, as well as the main references concerning the campaigns and the analyzed cases.

3. Sodar data reduction

Observations used in the present study were provided from the sodar developed in CRPE, which was operating during all four campaigns already mentioned. The CRPE sodar (described by Baudin et al. 1976) consists of a system of three monostatic antennas: one vertical and two slanting at 30° from the vertical. The angle of the horizontal projection is 90°. The acoustic pulse lasts 100 ms, the pulse repetition rate is 4 s, and the emission frequency is 2000 Hz. As it was pointed out by Spizzichino (1974), the antenna axis elevation and the pulse duration are adequately chosen in order to minimize the wind measurement errors. This Doppler sodar gives real-time data of Doppler frequency shift, and reflectivity of the backscattering intensity at each height level, that is, from 19 up to about 360 m over the ground and with a height resolution of 15 m.

TABLE 1. General presentation of the experimental campaigns.

Campaign Case study	Scientific goals Experimental site	Canopy/relief	Main references
MESOGERS84 28 September 1984	Dynamics of the boundary layer over complex terrain. Gers (France) (Fig. 1, box 1)	agricultural crops and trees/small hills and valleys	Weill et al. 1988a Ralph et al. 1993
HAPEX–MOBILHY86 4 June 1986	Hydrological balance over various canopies (forest/agricultural crops). Landes (France) (Fig. 1, box 2)	agricultural crops and pine forest/flat ground	André et al. 1988 Mazaudier and Weill 1989
FRONTS87 9–10 January 1988 12–13 January 1988	Dynamics of active cold fronts over northwestern Europe. English Channel (France–England) (Fig. 1, box 3)	bare soil, isolated trees/flat ground	Clough 1987 Thorpe and Clough 1991 Lagouvardos et al. 1992
PYREX90 15 October 1990	Dynamic influence of a large mountain range over the atmosphere. Pyrenees (France–Spain) (Fig. 1, box 4)	bare soil/mountain	Bougeault et al. 1990 Bougeault et al. 1993

In the following we shall describe the method used to estimate the momentum fluxes and friction velocity in the surface layer, using the 4-s time-resolution sodar data. Friction velocity was calculated from the data of the second gate of the Doppler sodar ($z = 34$ m). The surface-layer thickness varies, from some meters during stable conditions to 50 m, or even more, during neutral or unstable conditions. In this study, the interest is focused on cold-front passages, when strong winds and unstable conditions seem to confirm that $z = 34$ m is within the surface layer.

Files of the Doppler frequency shift measured every 4 s were available. For each one of the antennas, the radial wind speed can be obtained, as follows:

$$V_r = -\frac{c}{2}\frac{\Delta f}{f_0}, \tag{1}$$

where V_r is the radial velocity, c the sound speed, f_0 the emission frequency (=2000 Hz), and Δf the Doppler shift.

From the radial wind speeds, the three wind components u, v, w can be obtained in an orthogonal coordinate system. The fluctuations of the three wind components were calculated from the differences between the mean speed of the flow during the averaging period (10 min) and the instantaneous values. The trend of the mean speed with time was taken into account using a linear least-squares method over the ensemble of each sample. Then the correlation function of the signals u', w', ($C_{u'w'}$), as well as v', w', ($C_{v'w'}$), (u', v', w' being the fluctuations of the three wind components) were computed. Applying the method over a time period of 10 min, the fluxes $\langle u'w' \rangle$ and $\langle v'w' \rangle$ were obtained and then friction velocity was calculated from its definition formula:

$$u_* = [\langle u'w' \rangle^2 + \langle v'w' \rangle^2]^{1/4}. \tag{2}$$

A running average was performed so as to smooth the data. This analysis of 10-min time series of the sodar data, covers the frequency range 0.0017–0.125 Hz,

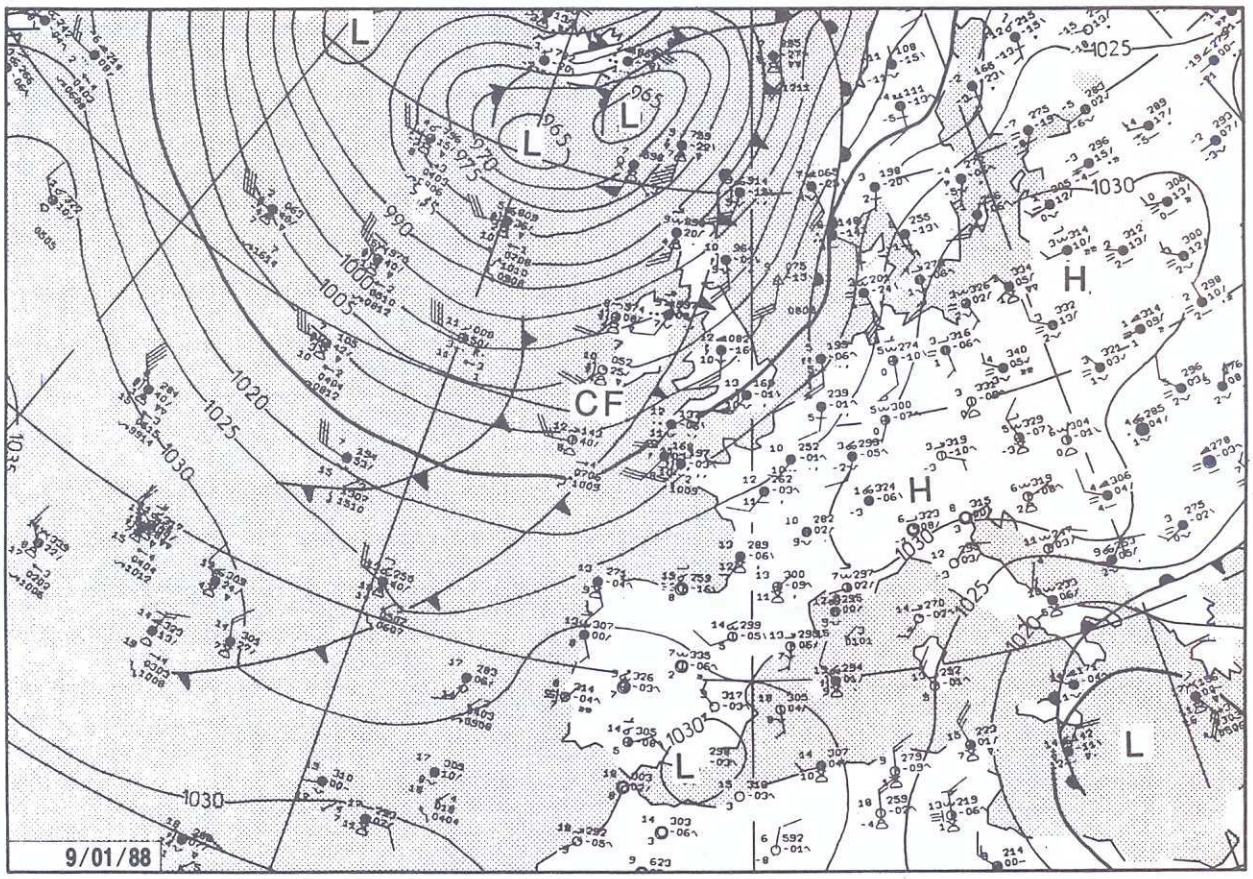

FIG. 2. Surface analysis of the synoptic situation at 1200 UTC 9 January 1988, 7 h prior to the frontal passage over the experimental area (from the Weekly Bulletin of the French Meteorological Service).

whereas the high-frequency part of the spectrum is cut off. From the theoretical $u'w'$ cospectra, under unstable conditions given in Kaimal et al. (1972), and the observed mean winds in our cases, one may conclude that the frequency range of the sodar data contains a large (and the most energetic) part of the production as well as a small part of the inertial subrange. So a small part of the high-frequency information is not included in friction velocities calculated in this study and therefore they are more representative of the low frequency part of the spectrum.

The routine treatment of the sodar data provided us with 15-min time-resolution data of the horizontal wind speed and vertical velocity, so it was possible to compare the time variation of the horizontal wind speed with that of the friction velocity in the surface layer. This comparison between horizontal wind speed and friction velocity for different case studies will be presented in the following section.

4. Observations

For each one of the four campaigns, cold-front cases have been selected and the variation of frontal friction has been compared to the time variation of horizontal wind speed. At first, we present the cases of two cold fronts observed during the FRONTS87 experiment that are our reference cases because the experimental area was free of complications due to irregular terrain conditions. In fact it was one of the aims of this campaign to study cold fronts propagating over a flat, bare ground which presents no, or minor, terrain effects. The second case refers to a cold-front system observed during the PYREX90 experiment where the terrain slanting and the nearby mountain range make their signature very evident on the time variation of friction velocity. The third case is a cold front over a forested area and occurred during the HAPEX–MOBILHY86 campaign. Finally, the last case refers to a front observed during the MESOGERS84 campaign over a heterogeneous crops terrain.

a. FRONTS87 case studies

From this campaign we are interested in two frontal cases, which correspond to two intensive observational periods (IOPs): the IOP 7 and IOP 8. Both cases refer to active cold fronts propagating over a flat terrain.

1) FRONTS87 IOP 7

On 9 January 1988 (IOP 7), a cold front traversed Brest fairly steadily at 7 m s^{-1} from 315° at 1900 UTC. The surface analysis (Fig. 2) of this day at 1200 UTC shows that the cold front was associated with a 965-hPa low centered in the north of the British Isles. Ahead of the front, in northwestern France, the flow was southwesterly, while west of the front, the flow had more of a westerly component. At the surface, the frontal passage was accompanied by a 2.5°C drop in surface temperature, a 70° veer, and a 5 m s^{-1} decrease in surface wind (for a detailed discription of this front see Thorpe and Clough 1991 and Lagouvardos et al. 1992). Time–height distribution of the alongfront wind component as well as the potential temperature have been constructed using data of 11 soundings released at Brest and are presented in Figs. 3a and 3b (the hours in the time scale are relative to the surface frontal passage at the site). This number of soundings corresponds to a 30-h time interval. A low-level jet (LLJ) with a horizontal extension of about 250 km and a maximum exceeding 24 m s^{-1} (situated at $z \approx 1$ km) was associated with this front. A strong cross-front gradient of the alongfront wind component characterized the frontal discontinuity, and it was accompanied by a strong gradient of the potential temperature θ field

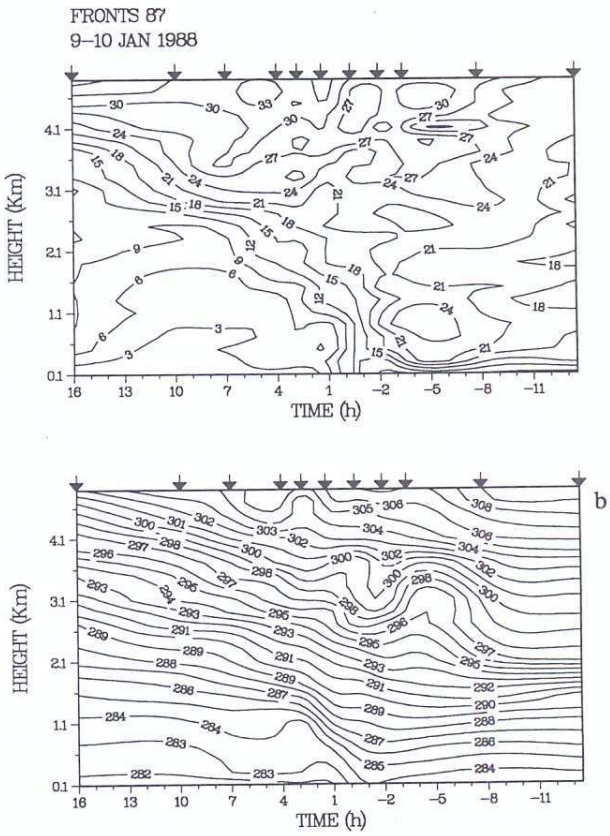

FIG. 3. Time–height cross sections of (a) the alongfront wind component with isotachs at intervals of 3 m s^{-1} and (b) the potential temperature with isentropes at intervals of 1 K, constructed from 11 soundings released from Brest airport. The hours on the time scale are relative to the passage of the front over Brest at 1900 UTC 9 January 1988. Arrows at the top of the diagram show the time of the sounding releases.

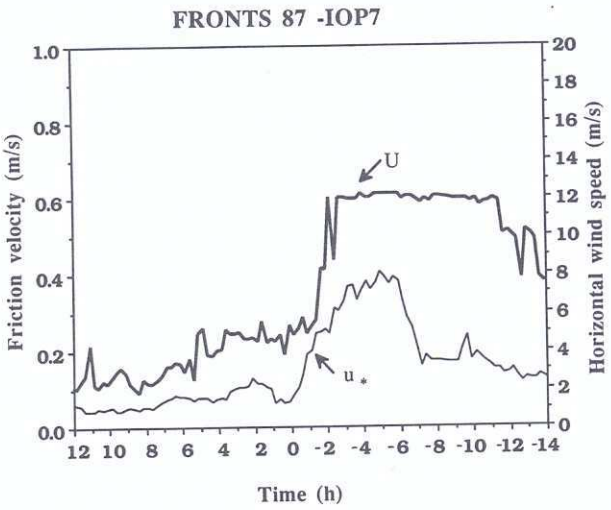

FIG. 4. Time variation at z = 34 m (second range gate of the sodar) of horizontal wind speed and friction velocity. The hours in the time scale are relative to the passage of the front over Brest (1900 UTC 9 January 1988).

separating the warm and cold sector. The warmest air of all in the prefrontal region, having originated farthest south, is found immediately ahead of the surface cold front (slightly increasing θ in the warm sector near the frontal discontinuity), in accordance with observations reported by Browning (1985). The LLJ is a kind of jet stream of moist air in the lower troposphere, between 100 and 1000 km wide and a few kilometers deep, ahead of midlatitude surface cold fronts. The detailed mesostructure and dynamics of this kind of jet in relation to their larger-scale environment has been studied by Browning and Harrold (1970) and Browning and Pardoe (1973), among others.

On the time variation of the horizontal wind speed and friction velocity, calculated from the Doppler sodar in the surface layer (at z = 34 m), the following characteristics can be seen (Fig. 4):

- The horizontal wind speed at z = 34 m (hereafter U) has a maximum magnitude of 12 m s^{-1} over a time period of about 10 h before the frontal passage and

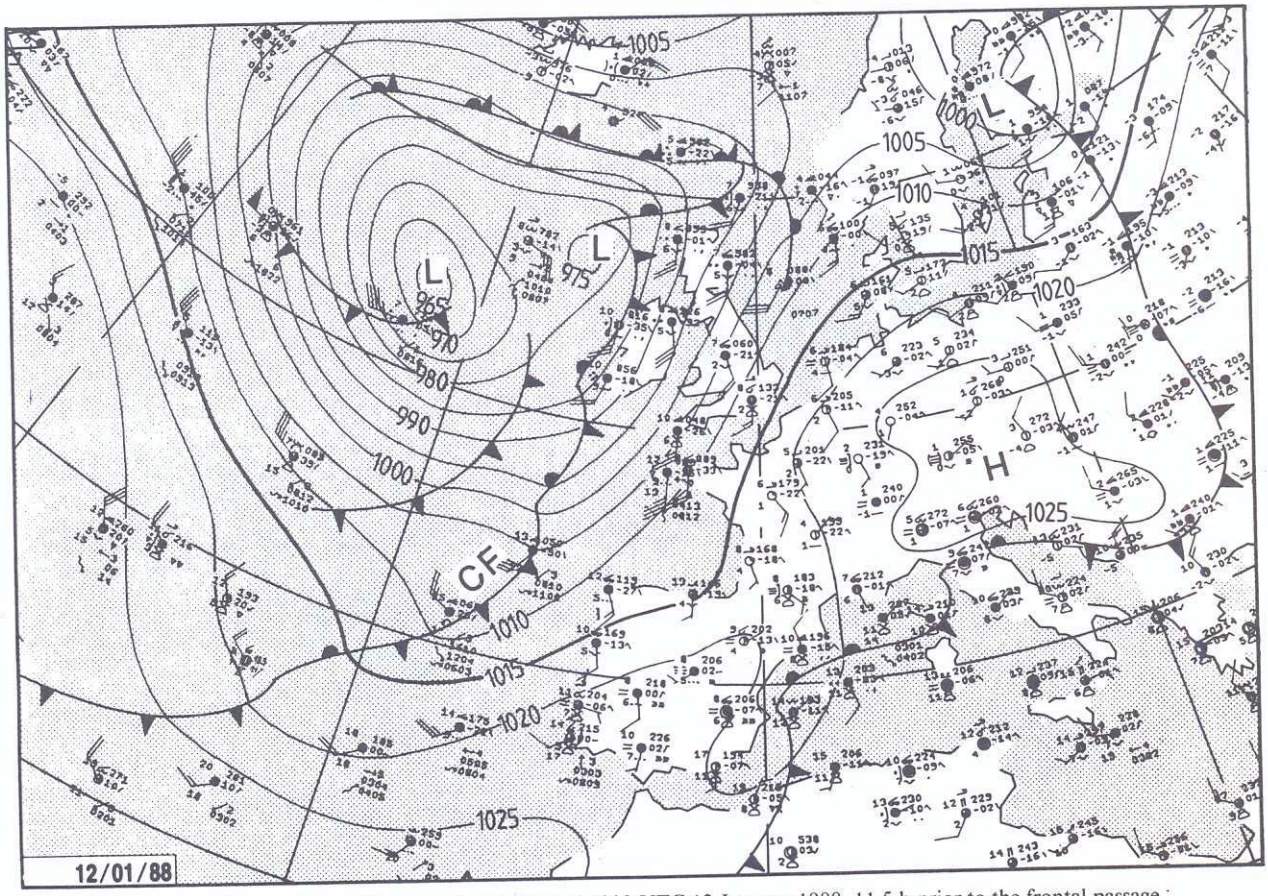

FIG. 5. Surface analysis of the synoptic situation at 1200 UTC 12 January 1988, 11.5 h prior to the frontal passage over the experimental area (from the Weekly Bulletin of the French Meteorological Service).

decreases right after the frontal passage (at 1900 UTC) down to 5 and then to 4 m s^{-1}.

- Friction velocity shows an increasing tendency during the time interval of stable U magnitude and more precisely during the time interval of the LLJ presence (about 10 h) as it was observed from the sounding data (Fig. 3a). The starting value of u_* is 0.15 m s^{-1} and it reaches a maximum of 0.4 m s^{-1} in the cold side of the LLJ. Friction-velocity maximum coincides with the most intense vertical shear under the LLJ maximum (at −5 h in Fig. 3a).
- Friction velocity diminishes simultaneously with the horizontal wind speed, right after the frontal passage.

2) FRONTS87 IOP 8

The next case study concerns the cold front of 12 January 1988, which traversed Brest at 6 m s^{-1} from 300°, at 2330 UTC; this case is documented by Thorpe and Clough (1991) and Lagouvardos et al. (1992). The synoptic situation characterizing this front can be seen on the surface analysis of 1200 UTC 12 January (Fig. 5). The cold front was associated with a 975-hPa low, situated in the northwest of Ireland. Satellite imagery showed evidence of a wavelike structure of the front (not shown). At the surface, the stations recorded a temperature drop of about 1°C after the frontal passage, a 90° veer, and a 7 m s^{-1} decrease in surface wind. Heavy rain accompanied the frontal passage for a 20-min time interval. As it concerns wind measurements by the sodar during precipitation, an elimination in real time based on signal-to-noise ratio was performed. As it was pointed out by Weill et al. (1988b), however, heavy precipitation affects wind measurements above the 200-m height.

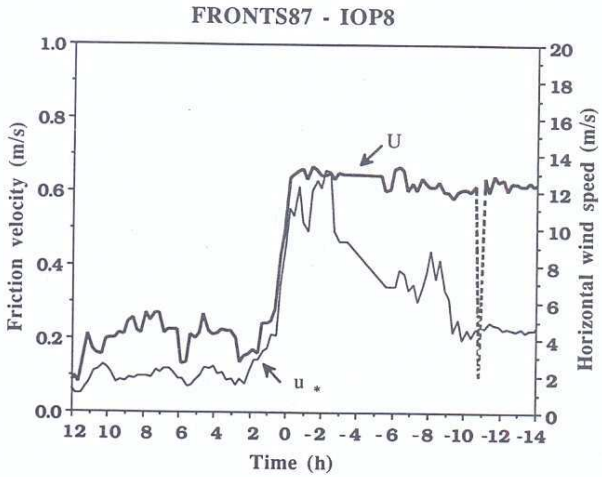

FIG. 7. Time variation at z = 34 m of horizontal wind speed and friction velocity. The hours in the time scale are relative to the passage of the front over Brest (2330 UTC 12 January 1988).

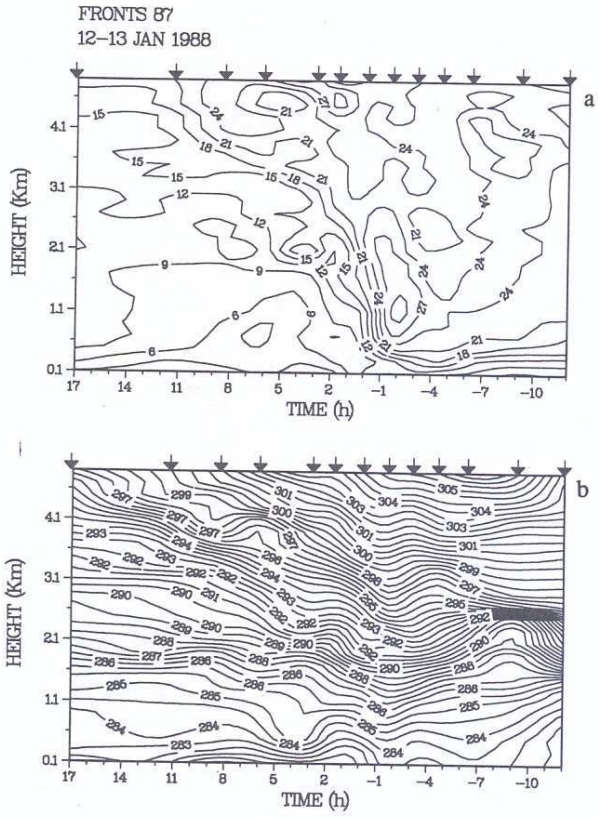

FIG. 6. Time–height cross sections of (a) the alongfront wind component with isotachs at intervals of 3 m s^{-1} and (b) the potential temperature with isentropes at intervals of 1 K, constructed from 13 soundings released from Brest airport. The hours on the time scale are relative to the passage of the front over Brest at 2330 UTC 12 January 1988. Arrows at the top of the diagram show the time of the sounding releases.

In the time–height cross sections (Figs. 6a,b) constructed from the soundings (13 ascents during the 29-h period presented), it can be observed that the front was associated with a strong cross-front gradient of the alongfront wind component. A strong but very narrow LLJ (compared to the IOP 7 case) is also evident, with a horizontal extension of about 100 km, a maximum situated at a height of about 1100 m, and exceeding 30 m s^{-1}. The signature of the front on the potential temperature field is very weak. The last characteristic constitutes a major difference compared to the previous case where the frontal passage was accompanied by a strong gradient of the potential temperature (Fig. 3b).

On the time variation of the horizontal wind speed and friction velocity presented in Fig. 7, one can observe, qualitatively, the same behavior as in the previous case, with some differences from a quantitative point of view:

• Here U is stable over a long period before the frontal passage (14 h or more) with a magnitude of 12 m s^{-1} and decreases abruptly after the frontal passage to 4–5 m s^{-1}.

• Friction velocity shows an increase, especially during the time period of the LLJ presence, starting from a value of 0.3–0.4 m s^{-1} and reaching 0.65 m s^{-1} under the LLJ maximum. Friction-velocity maximum coincides with the region of the most intense vertical shear under the LLJ maximum (at −2.5 h in Fig. 6a).

• Friction-velocity response to the sudden decrease of U after the frontal passage is simultaneous.

It must be remarked that although in this case the horizontal wind speed has the same stable maximum value as in the IOP 7 case study, friction velocity is more intense. One may assume that as the terrain conditions and the mean flow direction before the frontal passage were almost the same, the more intense friction velocity in the surface layer is directly related to the more pronounced LLJ of the last case study. Another remark, for both cases, is that the maximum of friction velocity is situated in the cold side of the LLJ (on the left of its core). This observation is in good agreement with Mak's (1972) numerical model results, concerning LLJ in midlatitudes, where he argued that friction should be more intense in the cold side of the LLJ.

Therefore, the relation between friction velocity and the LLJ presence seems to deserve further investigation in the future; the analysis of more cases would provide statistical results of the relation of LLJ and friction velocity in the surface layer.

b. The PYREX case study

During this experiment the Doppler sodar was situated at Lannemezan in the southwest of France at a slanting site in the north of the Pyrenees Mountains (Fig. 1). This case study (IOP 3 of the PYREX experiment) refers to the frontal passage of 15 October 1990. This case was principally selected for its associated lee-wave activity. Figure 8 shows the surface analysis at 1200 UTC 15 October. There exists a large depression zone over the Atlantic associated with a 990-hPa minimum extending from the north of Ireland to the west of Brittany. The cold front associated with this

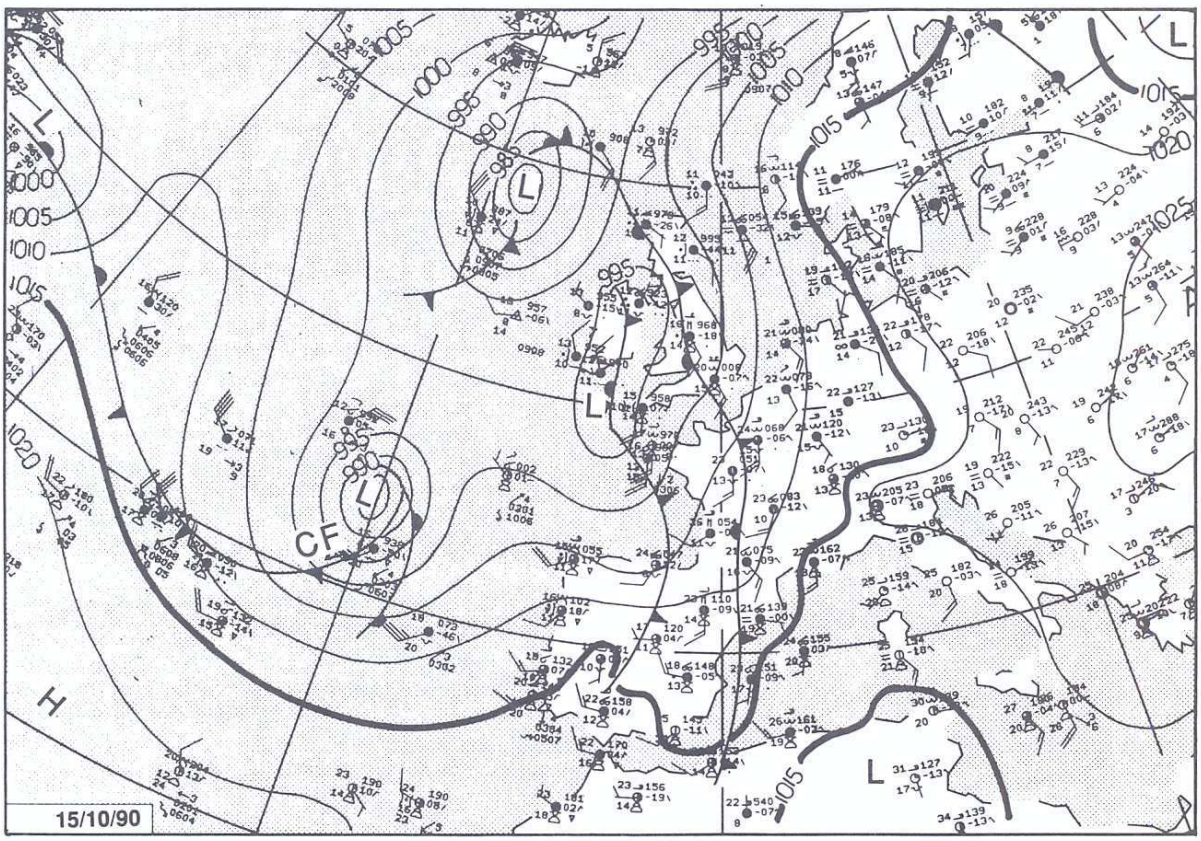

FIG. 8. Surface analysis of the synoptic situation at 1200 UTC 15 October 1990, 1 h prior to the frontal passage over the experimental area (from the Weekly Bulletin of the French Meteorological Service).

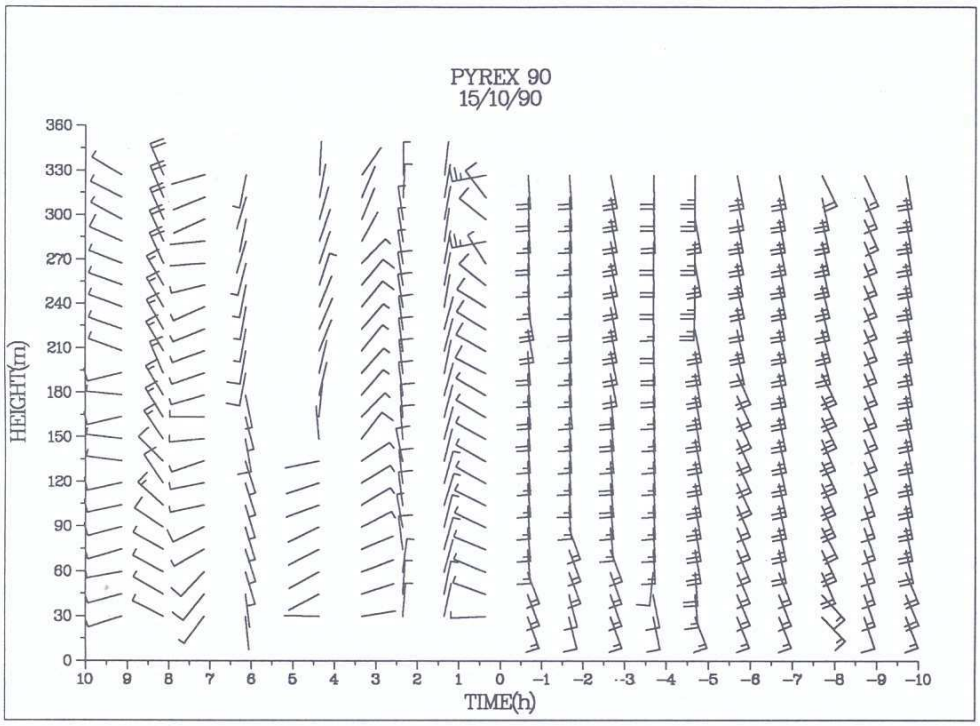

FIG. 9. Fifteen-minute average of the horizontal wind measured by sodar (for each hour, one profile over four is shown). Full barb—5 m s^{-1}, half-barb—2.5 m s^{-1}. The hours are relative to the passage of the front over Lannamezan, at 1300 UTC 15 October 1990.

minimum reached the experimental area near 1300 UTC; the synoptic flow in front of it is from south-southwest. Since soundings measurements are not available in the vicinity of the sodar site, the frontal passage is mainly documented by the sodar. Figure 9 presents 15-min-averaged profiles of horizontal wind speed measured by the sodar (for graphic clarity one profile over four is shown). It can be seen that the frontal passage was accompanied by a remarkable veering from south to west-northwest and then to north before stabilizing to a westerly component, together with a decrease of 5 m s^{-1} of the horizontal wind speed. The same remarkable change in wind direction was independently measured from the surface stations (not shown). It is beyond the scope of this paper to investigate the reasons of this highly variating wind direction after the frontal passage, but it could be due to orographic gravity waves.

From the time variation of the horizontal wind speed and friction velocity shown in Fig. 10, the following characteristics can be observed:

- The horizontal wind speed has an oscillating magnitude of around 7 and 8 m s^{-1} before the frontal passage, and decreases down to 3–4 m s^{-1} after it.
- Friction velocity has strong and oscillating values before the frontal passage with a fairly increasing trend, starting from values around 0.6 m s^{-1} and reaching

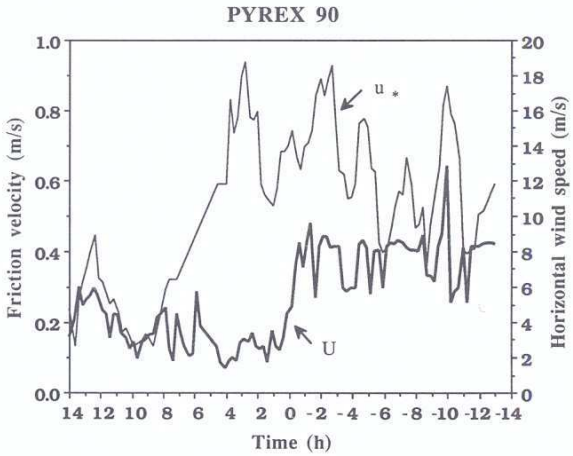

FIG. 10. Time variation at z = 34 m of horizontal wind speed and friction velocity. The hours in the time scale are relative to the passage of the front over Lannemezan (1300 UTC 15 October 1990).

values around 0.8–0.9 m s^{-1}, that is, the most intense values compared to all other cases.

- Friction velocity does not decrease simultaneously with the sudden decrease of horizontal wind speed after the frontal passage but shows a delay of more than 6 h.

The last characteristic is associated with the abrupt changes of the wind direction, which last almost 7 h, as is already mentioned (Fig. 9). These different wind directions induce different roughness conditions and explain the inertia in the decrease of friction velocity after the frontal passage. The high values of friction velocity corresponding to less intense values of U than in the previous cases are associated with the terrain features. In sodar facsimile records (covering 0–500 m), downward oscillating layers due to wave activity are evident during 4 h after the frontal passage (not shown). At the time of the u_* maximum, these layers are confined in the first 100 m.

The cases presented before (IOP 7, IOP 8, of FRONTS87) were cases over a nearly flat terrain, properly chosen such as not to have topographic effects interfering in the frontal dynamics. On the contrary, the IOP 3 of the PYREX experiment was a case over a slanting terrain near a mountain range where wave-like activity often occurs (Bougeault et al. 1990). Indeed, as it was reported by Bougeault et al. (1993), in the presence of the Pyrenees, the southerly airflow observed during this case study generated lee waves giving four main regions of ascending motions parallel to the mountain range. As the sodar site was at the lee side of the mountain, wave activity yields a superposition of an oscillating behavior on the friction velocity time variation.

c. *The HAPEX–MOBILHY case study*

During the intensive observational phase of the HAPEX–MOBILHY experiment, the CRPE sodar was routinely operated at Estampon (Fig. 1), a forested site composed of pine trees averaging 19 m in height.

This case study concerns the frontal situation that occurred on 5 June and traversed the experimental area at about 1400 UTC from 0°. A surface analysis map is presented in Fig. 11. A surface cold front was present

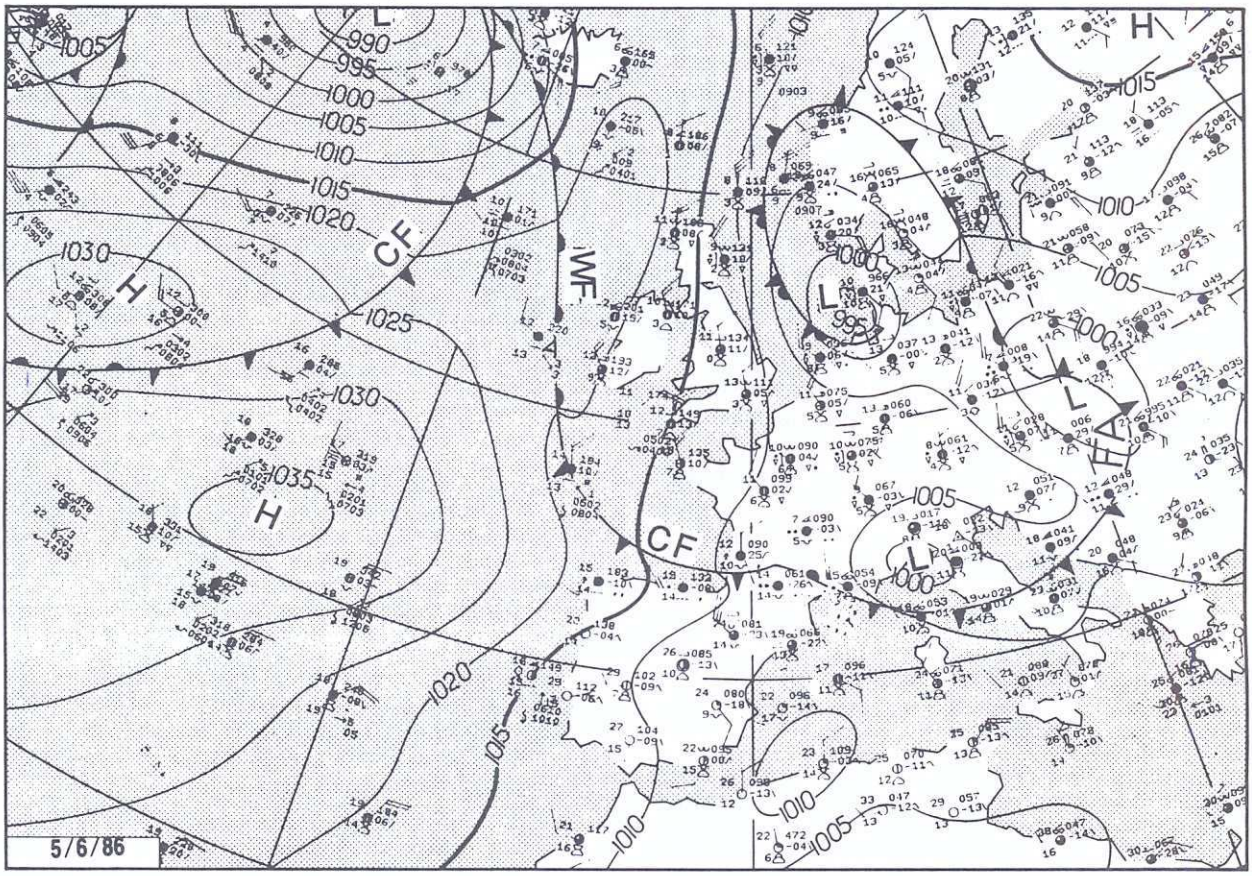

FIG. 11. Surface analysis of the synoptic situation at 1200 UTC 5 June 1986, 2 h prior to the frontal passage at the experimental area (from the Weekly Bulletin of the French Meteorological Service).

over southern France while a surface anticyclone was building into the region to the west of the front. The low-level flow was from the west ahead of the front and from the north behind it. The frontal propagation was apparently blocked by the Pyrenees Mountains and therefore the front was slipping to the southeast instead of to the south. The frontal passage was associated with a 2°C decrease of temperature, a 120° veer, and a 3 m s^{-1} decrease of the horizontal wind speed. From the sounding data (nine ascents during the 34-h time interval presented), the time–height cross sections of the potential temperature and alongfront wind component have been constructed (Figs. 12a,b). It can be observed that the cross-front gradient of the alongfront wind component was accompanied by a cross-front gradient of the potential temperature field; an LLJ is also present with a maximum situated at 1300 m, which exceeds 18 m s^{-1}. That is a less pronounced LLJ than those already presented. It should be noted that the cross-front gradient of the alongfront wind component appears less intense than in the previous cases. In fact, the cross sections presented are not in a direction perpendicular to the frontal discontinuity but more in a diagonal direction, as the front is apparently slipping along its surface. Thus, the experimental area is within the frontal discontinuity for a longer period and measurements are performed into the cold sector nearly 4 h after 1400 UTC (1400 UTC corresponds to 0 h in the time scales of Figs. 12–14).

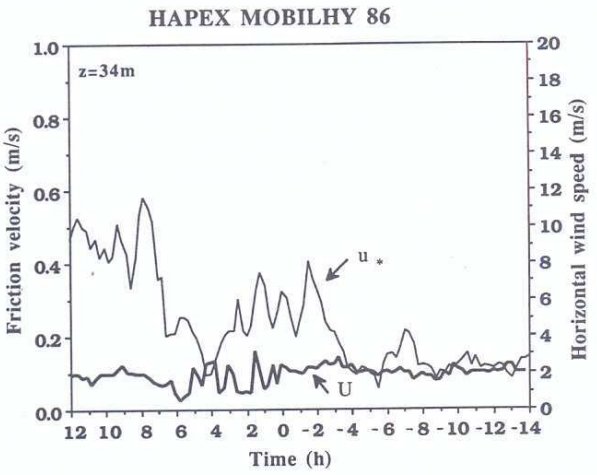

FIG. 13. Time variation at z = 34 m of horizontal wind speed and friction velocity. The hours in the time scale are relative to the passage of the front over the experimental area (1400 UTC 5 June 1986).

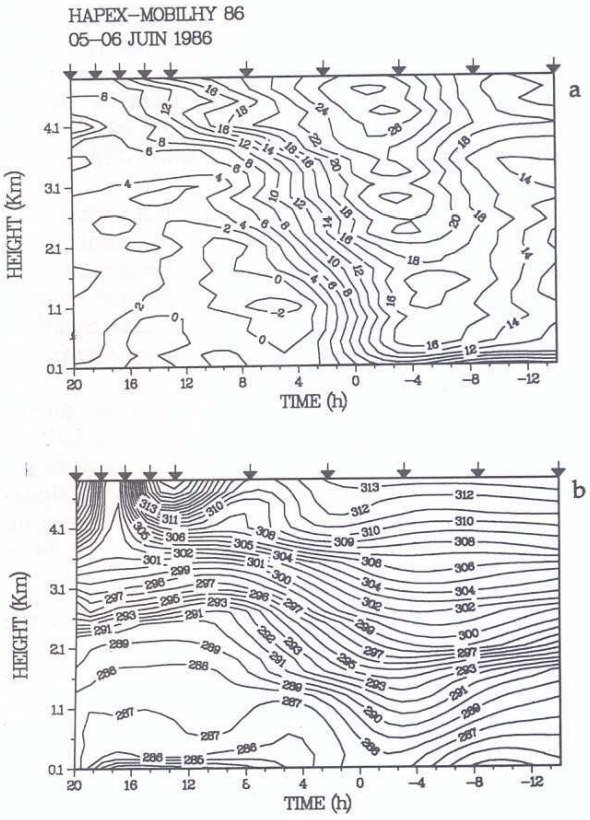

FIG. 12. Time–height cross sections of (a) the alongfront wind component with isotachs at intervals of 2 m s^{-1} and (b) the potential temperature with isentropes at intervals of 1 K, constructed from ten soundings. The hours on the time scale are relative to the passage of the front over the experimental area on 5 June 1986 (1400 UTC). Arrows at the top of the diagram show the time of the sounding releases.

Figures 13 and 14 show the time variation of horizontal wind speed and friction velocity at 34 and at 63 m, respectively. It can be seen that

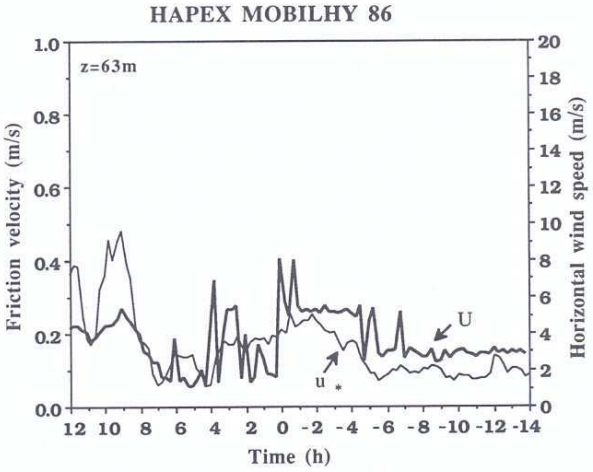

FIG. 14. As in Fig. 13 but at z = 63 m (fourth range gate of the sodar).

• The signature of the front on the time evolution of horizontal wind speed is not present at $z = 34$ m (see Fig. 13) but is present at 63 m (decrease of U at 0 and 4 h on the time scale of Fig. 14).

• There exists a strong vertical shear between 34 and 63 m especially after the frontal passage (such a strong shear was not present in the previous cases).

• The frontal signature, although not present at $z = 34$ m on the wind time variation, exists in the friction-velocity time evolution. Before the frontal passage, u_* is about 0.1 m s^{-1}, then shows an increase, reaching values of about 0.3 m s^{-1}, and at last decreases instantaneously at +4 h. The same variation is also present at 63 m, where, at about 6 h before the frontal passage, u_* begins to increase, starting from 0.1 m s^{-1} and reaching 0.25 m s^{-1}, and then to decrease instantaneously after the end of the frontal passage.

• After the end of the frontal disturbance at +4 h (that is at 1800 UTC), one can see that friction velocity becomes very intense although U remains constant (about 2 m s^{-1}). High values of local friction velocity are also present at 63 m, corresponding to an increasing wind at the same level.

These intense values of u_* can be explained by

(a) the existence of strong shear between 34 and 63 m (the vertical momentum fluxes are proportional to the horizontal wind speed vertical gradient),

(b) the change of wind direction to a wind from west (u_* is related to the magnitude and direction of horizontal wind speed), and

(c) the frictional effect due to the forest.

In fact, Mazaudier and Weill (1989) have shown for the same experiment that forest frictional effects depend on the wind regime (magnitude and direction) and that some wind directions yield to more intense frictional effects. In their study they used a displacement height $d = 0.8h$, h being the height of the vegetation (19 m). They also noted that the transition between the forest surface layer and the forest boundary layer is sharp and that a wind shear between 34 and 63 m is very often observed.

d. The MESOGERS84 case study

This case study refers to the cold front of 29 September 1984, documented by Ralph et al. (1993). The synoptic situation at 1800 UTC is shown in Fig. 15. Ahead of the front, the flow was southerly, while west of the front, the flow had a more westerly component. The temperature drop across the front, as it was recorded from the ground stations, was about 3°C. The front had a propagation speed of 10 m s^{-1} from the west and reached the MESOGERS area at 1900 UTC. Ralph et al. (1993) reported that ahead of the front there was some indication of an LLJ. The frontal passage was observed by the sodar as a horizontal wind shift of almost 180° and a 7 m s^{-1} decrease (Fig. 16). It had been suggested by Ralph et al. (1993), that this case is a cold-front scale contracted to a gravity current.

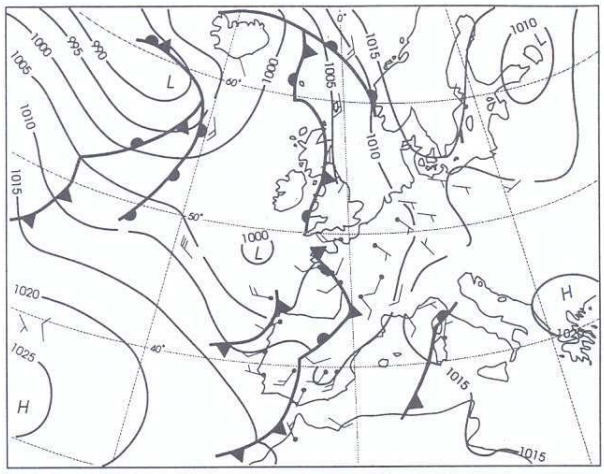

FIG. 15. Surface analysis of the synoptic situation at 1800 UTC 28 September 1984, 1 h prior to the frontal passage over the experimental area.

The time variation of horizontal wind speed U and friction velocity, at $z = 34$ m, are displayed in Fig. 17. One can see that

• The signature of this front on the horizontal wind speed is very brief, corresponding to the contraction of the front to a gravity current. The horizontal wind speed U, increases from 3 m s^{-1} to 10 m s^{-1} within an hour and then decreases within less than a half an hour to about 3 m s^{-1}. After the frontal passage, the wind reaches values around 2 m s^{-1}.

• Friction velocity shows a small increase during the time interval of the wind increase, from 0.05 to 0.14 m s^{-1}, and then a slight decrease to 0.06 m s^{-1} after the frontal passage, but indeed the frontal signature is very weak. This signature is more intense on the time variation of the local u_* at 49, 63, and 74 m (not shown).

At the synoptic scale, this case is different from the previous ones. The surface front disturbance is very brief and this fact can also explain the weakness of the frontal signature in the friction-velocity time variation.

Table 2 summarizes the principal characteristics of each one of the selected cases at the surface: the time of the frontal passage, its propagation speed and direction, and the decrease of the surface wind and temperature associated with the frontal passage.

5. Discussion

For presentation clarity, the principal observations and morphological features corresponding to each one

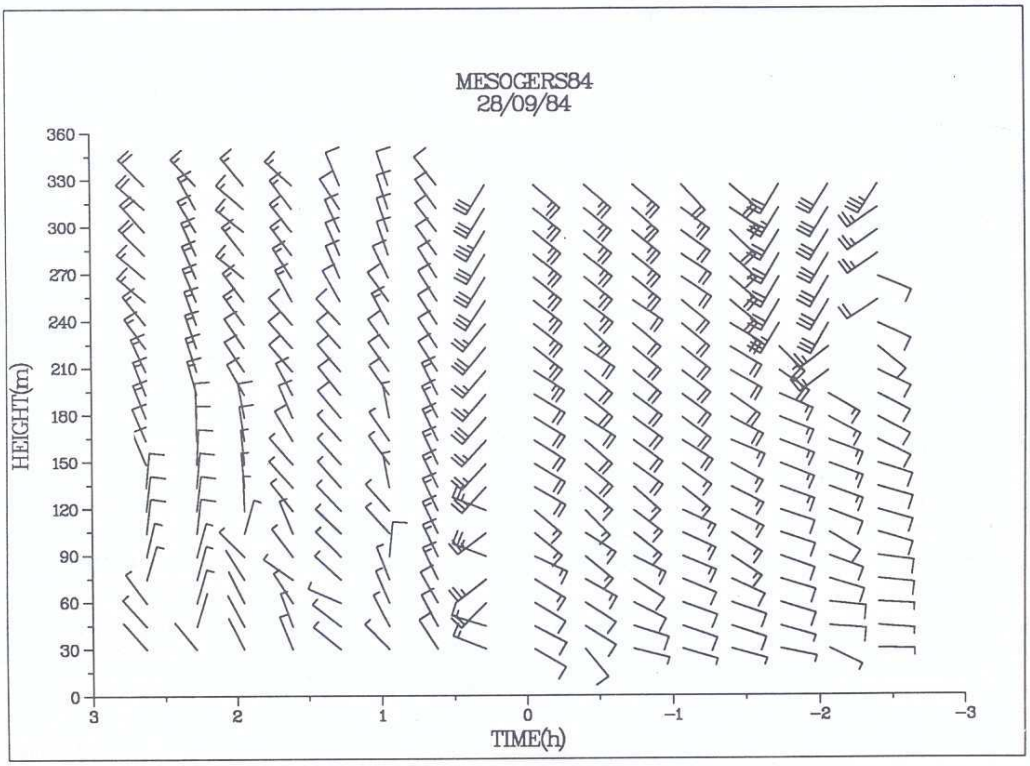

FIG. 16. Twenty-minute average of the horizontal wind measured by sodar. Full barb—5 m s^{-1}, half-barb—2.5 m s^{-1}. The hours are relative to the passage of the front over the experimental area, at 1900 UTC 28 September 1984.

of the cases are put together in Table 3, and the resulting remarks can be summarized in the following.

Whatever the terrain characteristics are, the signature of a frontal passage consists of an increase of friction velocity some hours before the frontal passage and a quick and sudden decrease just at the frontal occurrence or some hours after it. When the data allowed to put in evidence the LLJ associated with the frontal passage, it is observed that

- u_* increases in the presence of the LLJ,
- the u_* maximum value is situated beneath the cold sector of the LLJ, and
- the u_* maximum value represents about 2% of the amplitude of the LLJ.

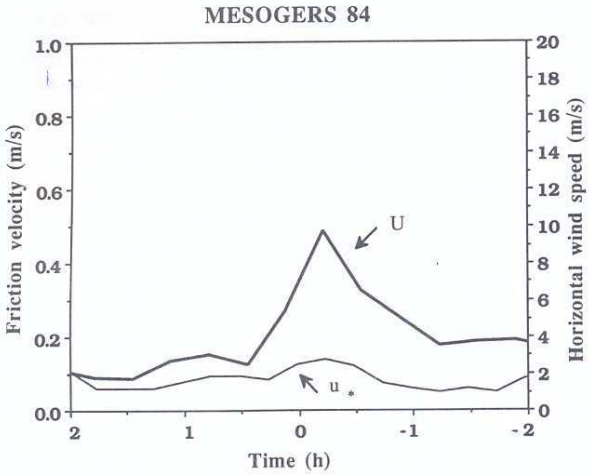

FIG. 17. Time variation at z = 34 m of horizontal wind speed and friction velocity. The hours in the time scale are relative to the passage of the front over the experimental area (1900 UTC 28 September 1984).

The topography influences in various ways. In the case of the presence of a mountain and a slanting terrain (PYREX90 case study), more intense u_* values are observed. When lee waves (due to the mountain) are observed, an oscillation is superposed on the friction-velocity variation. In the presence of a forest (HAPEX–MOBILHY86 case study), the signature already described is observed at higher altitudes. This can be explained by the fact that the average height of the trees being 19–20 m, the surface layer does not extend from the ground up to some tens of meters but begins at about 20 m. Stability conditions are also very important in modulating friction velocity and its relation with horizontal wind speed in the surface layer. Nevertheless, strong winds before the frontal passage

TABLE 2. Characteristics of each frontal case at the surface.

Campaign Case study	Time of frontal passage (UTC)	Front propagation speed/propagation direction	Wind rotation after the frontal passage	Wind speed decrease ($m\ s^{-1}$)	Temperature decrease (°C)
FRONTS87 IOP 7 9–10 January 1988	1900	7 $m\ s^{-1}$/315°	70°	5	2.5
FRONTS87 IOP 8 12–13 January 1988	2330	6 $m\ s^{-1}$/300°	90°	7	1
PYREX90 IOP 3 15 October 1990	1300	—/260°	180°	5	—
HAPEX–MOBILHY86 5 June 1986	1400	—/0°	120°	3	2
MESOGERS84 29 September 1984	1900	10 $m\ s^{-1}$/300°	180°	7	3–4

result in homogenizing the surface layer, so dynamic processes dominate the frontal signature on friction velocity variation especially before the frontal passage.

Figure 18 represents the relation among the LLJ presence, friction velocity, and horizontal wind speed in the surface layer, as it can be summarized from the

TABLE 3. Summary of the observations on the wind field at different layers and morphological features resulting from the frontal passage for each case study. The u_{*l} and u_{*m} denote friction velocity before the frontal passage and friction-velocity maximum, respectively, U_1 and U_2 horizontal wind speed at 34 m before and after the frontal passage, U_{LLJ} the maximum of the low-level jet.

Campaign Case study	u_{*l} u_{*m} ($m\ s^{-1}$)	U_1 U_2 ($m\ s^{-1}$)	U_{LLJ} ($m\ s^{-1}$)	u_{*m}/U_{LLJ}	Morphological features at 34 m
FRONTS87 IOP 7 9–10 January 1988	0.15 0.4	12 4–5	>24	1.7%	• u_* increases several hours before the frontal passage (10 h), while U remains constant • U and u_* decrease simultaneously with the frontal passage
FRONTS87 IOP 8 12–13 January 1988	0.3–0.4 0.65	12 4–5	>30	2.1%	• same signature as for the preceeding case but with more intense values of u_*
PYREX90 IOP 3 15 October 1990	0.6 0.8–0.9	7–8 3–4	?	?	• oscillating values of u_* • U decreases simultaneously with the frontal passage • u_* decreases several hours after the frontal passage
HAPEX–MOBILHY86 5 June 1986	0.1 0.3	6 2–3	>18	1.7%	• same signature as for cases 1 and 2 but shifted at a higher altitude (63 m)
MESOGERS84 29 September 1984	0.05 0.14	10 3	?	?	• u_* and U change simultaneously (increase and decrease)

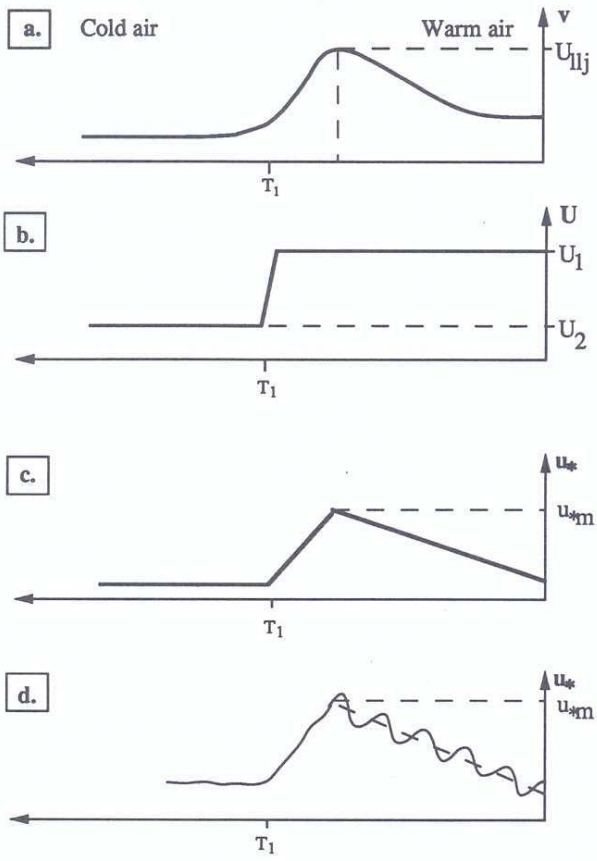

FIG. 18. Schematic representation of the time variation of (a) the alongfront wind component v, at the height of the LLJ maximum, (b) the horizontal wind speed in the surface layer, (c) the friction velocity in the surface layer, and (d) as in (c) but at a site near a mountain range. Here T_1 denotes the time of the frontal passage; U_{LLJ} the v maximum value; U_1, U_2 the magnitude of horizontal wind speed in the surface layer before and after the frontal passage; and u_{*m} the maximum value of friction velocity.

observations. Figure 18a presents schematically the time variation of the alongfront wind component v, at the height of the LLJ maximum (approximately at z = 1000–1100 m). It presents an increasing trend, reaches its maximum value (U_{LLJ}), and then decreases. The increasing and decreasing regions are not symmetric; the time of the frontal passage is denoted by T_1. The horizontal wind speed U in the surface layer (z = 34 m), presented in Fig. 18b, does not show the same time variation as v. In fact, U has a stable value (U_1) before the frontal passage and decreases abruptly after it. In Fig. 18c, friction velocity at the same level (z = 34 m) is represented. Although U has a stable value before the frontal passage, friction velocity shows a similar behavior with the alongfront wind component time variation (Fig. 18a) and reaches its maximum value, u_{*m}, simultaneously with the alongfront wind component. Friction-velocity values are more intense in the cold sector of the LLJ and decrease after the frontal passage. The frontal signature on friction velocity in the presence of a mountain is shown in Fig. 18d. The difference from Fig. 18c is that now u_* values are more intense and oscillating.

The cases presented in this paper show the interest of continuing, in the future, this study for more cases so as to manage to characterize "statistically" the various parameters relating the LLJ presence and friction velocity in the surface layer:

- the ratio between u_* and LLJ maximum values (u_{*m}/U_{LLJ}, see Table 3);
- the time (T_1) between the beginning of u_* increase and the frontal passage. This time interval could characterize the horizontal extension (E) of the turbulent region ahead of the frontal discontinuity, $E = VT_1$, where V is the propagation speed of the front;
- the rate of the increase of u_*, ($\Delta u_*/\Delta t$); and
- the horizontal extension of the LLJ.

The study of a large number of cases may allow an understanding of how all of these observed parameters are related, and if the value u_{*m}/U_{LLJ} = 2% found for the three cases is statistically valid.

6. Conclusions

The aim of this study was the analysis of the influence of topography on surface friction velocity during a frontal passage. Five frontal events have been studied using sodar and sounding data, and it has been shown that there is an almost constant frontal signature on friction velocity (summarized in Table 3 and Fig. 18). The characteristics of frontal friction, which are put into evidence in this paper, might be of some help in the understanding of the interactions between the PBL and a mesoscale disturbance, and perhaps be useful for numerical modeling parameterizations. This analysis concerned a limited number of case studies and it should be continued for a larger number of cases to obtain statistical results. In the future, with an operating network of three stratospheric–tropospheric (UHF) wind profilers and three sodars it should be possible to analyze and better understand the circulations related to the LLJ in relation to surface friction in three dimensions. The authors plan to undertake and present a similar study, but in two dimensions, using stratospheric–tropospheric (UHF) radar and sodar data available from the FRONTS87 experimental campaign.

Acknowledgments. Special thanks are attributed to Y. Lemaître for a lot of valuable comments on early versions of the manuscript. Thanks are also attributed to A. Weill for valuable discussions concerning sodar data reduction. Constructive comments of the review-

ers of this paper are also appreciated. The four experimental campaigns received support grants from INSU/PAMOS (Institut des Sciences de l'Univers/Programme Atmosphère Moyenne et Océan Superficiel), CNET (Centre National d'Etudes et des Télécommunications), and CNRS (Centre National de la Recherche Scientifique).

REFERENCES

André, J. C., J. P. Goutorbe, A. Perrier, F. Becker, P. Bessemoulin, P. Bougeault, Y. Brunet, W. Brutsaert, T. Carlson, R. Cuenca, J. Gash, J. Gelpe, P. Hildebrand, P. Lagouarde, C. Lloyd, L. Mahrt, P. Mascart, C. Mazaudier, J. Noilhan, C. Ottle, M. Payen, T. Phulpin, R. Stull, J. Shuttleworth, T. Schmugge, O. Taconet, C. Tarrieu, R. M. Thepenier, C. Valencogne, D. Vidal-Madjar, and A. Weill, 1988: Evaporation over land-surfaces: First results from HAPEX-MOBILHY special observing period. *Ann. Geophysicae,* **6**(5), 477–492.

Ball, F. K., 1960: A theory of fronts in relation to surface stress. *Quart. J. Roy. Meteor. Soc.,* **86,** 51–66.

Baudin, F., G. Belbeoch, and R. Chezlemas, 1976: Le sodar triple du CNET, Tech. Note CRPE/28, 135 pp [in french].

Bougeault, P., A. Jansa Clar, B. Benech, B. Carissimo, J. Pelon, and E. Richard, 1990: Momentum budget over the Pyrenees: The PYREX experiment. *Bull. Amer. Meteor. Soc.,* **71,** 806–818.

——, ——, J. L. Attie, I. Beau, B. Benech, R. Benoit, P. Bessemoulin, J. L. Caccia, B. Carissimo, J. L. Champeaux, M. Crochet, A. Druilhet, P. Durand, E. Elkhalfi, A. Genoves, M. Georgelin, K. P. Hoinka, V. Klaus, E. Koffi, V. Kotroni, C. Mazaudier, J. Pelon, M. Petitdidier, Y. Pointin, D. Puech, E. Richard, T. Satomura, J. Stein, and D. Tannhauser, 1993: The atmospheric momentum budget over a major mountain range: First results of the PYREX field program. *Ann. Geophysicae,* submitted.

Browning, K. A., 1985: Conceptual models of precipitation systems. *ESA J.,* **9,** 157–178.

——, and T. W. Harrold, 1970: Air motion and precipitation growth at a cold front. *Quart. J. Roy. Meteor. Soc.,* **96,** 369–389.

——, and C. W. Pardoe, 1973: Structure of low-level jet streams ahead of mid-latitude cold fronts. *Quart. J. Roy. Meteor. Soc.,* **99,** 619–638.

Businger, J. A., J. C. Wyngaard, Y. Ijumi, and E. F. Bradley, 1971: Flux-profile relationships in the atmospheric surface layer. *J. Atmos. Sci.,* **28,** 181–189.

Byun, D. W., 1990: On the analytical solutions of flux-profile relationships for the atmospheric surface layer. *J. Appl. Meteor.,* **29,** 652–657.

Clough, S. A., 1987: The mesoscale frontal dynamics project. *Meteor. Mag.,* **116,** 32–42.

Hoskins, B. J., and F. P. Bretherton, 1972: Atmospheric frontogenesis models: Mathematical formulation and solution. *J. Atmos. Sci.,* **29,** 11–37.

Kaimal, J. C., J. C. Wyngaard, Y. Izumi, and O. R. Côté, 1972: Spectral characteristics of surface layer turbulence. *Quart. J. Roy. Meteor. Soc.,* **98,** 563–589.

Keyser, D., and R. Anthes, 1982: The influence of planetary boundary layer physics on frontal structure in the Hoskins-Bretherton horizontal shear model. *J. Atmos. Sci.,* **39,** 1783–1802.

Lagouvardos, K., Y. Lemaître, and G. Scialom, 1992: Mesoscale ageostrophic circulations of two fronts observed during the FRONTS 87 experiment. Diagnosis and interpretation. *Meteor. Atmos. Phys.,* **48,** 293–307.

Lo, A. K., 1979: On the determination of boundary-layer parameters using velocity profile as a sole information. *Bound.-Layer Meteor.,* **17,** 465–484.

Mak, M. K., 1972: Steady, neutral planetary boundary-layer forced by a horizontally non-uniform flow. *J. Atmos. Sci.,* **29,** 707–717.

Mazaudier, C., and A. Weill, 1989: A method of determination of dynamic influence of the forest on the boundary layer using two Doppler sodars. *J. Appl. Meteor.,* **28,** 705–710.

Nieuwstadt, F., 1978: The computation of friction velocity u_* and the temperature scale T_* from temperature and wind velocity profiles by least square methods. *Bound.-Layer Meteor.,* **14,** 235–246.

Ralph, M., C. Mazaudier, M. Crochet, and S. V. Venkateswaran, 1993: Doppler sodar and radar wind-profiler observations of gravity-wave activity associated with a gravity current. *Mon. Wea. Rev.,* **121,** 444–463.

Spizzichino, A., 1974: Discussion of the operating conditions of a Doppler sodar. *J. Geophys. Res.,* **79,** 5585–5591.

Stone, P. H., 1966: Frontogenesis by horizontal wind deformation fields. *J. Atmos. Sci.,* **23,** 455–465.

Thorpe, A. J., and S. A. Clough, 1991: Mesoscale dynamics of cold fronts: Structures described by dropsoundings in FRONTS 87. *Quart. J. Roy. Meteor. Soc.,* **117,** 903–941.

Weill, A., C. Mazaudier, F. Baudin, C. Klapisz, F. Leca, M. Masmoudi, D. Vidal Madjar, R. Bernard, O. Taconet, B. S. Gera, A. Sauvaget, A. Druilhet, P. Durand, J. Y. Caneil, P. Mery, G. Dubosclard, A. C. M. Beljaars, W. A. A. Monna, J. G. Van Der Vliet, M. Crochet, D. Thomson, and T. Carlson, 1988a: The 'MESOGERS 84' experiment: A report. *Bound.-Layer Meteor.,* **42,** 251–264.

——, F. Baudin, C. Mazaudier, G. Desbraux, C. Klapisz, A. G. Driedonks, J. P. Goutorbe, A. Druilhet, and P. Durand, 1988b: A mesoscale shear convective cell observed during the COAST experiment: Acoustic sounder measurements. *Bound.-Layer Meteor.,* **44,** 359–371.